J. Phys. Chem. A **2001,** *105,* 169−183

Reactivity Dynamics in Atom−Field Interactions: A Quantum Fluid Density Functional Study

P. K. Chattaraj* and B. Maiti

Department of Chemistry, Indian Institute of Technology, Kharagpur 721302, India

Received: May 31, 2000; In Final Form: September 14, 2000

Dynamical behavior of chemical reactivity indices like electronegativity, hardness, polarizability, entropy, electrophilicity and nucleophilicity indices and uncertainty product is studied within a quantum fluid density functional framework for the interactions of a helium atom in its ground and excited electronic states with monochromatic and bichromatic laser pulses with different intensities. Time dependent analogues of various electronic structure principles like the principles of electronegativity equalization, maximum hardness, minimum polarizability and maximum entropy have been found to be operative. Insights into the variation of intensities of the generated higher order harmonics on the color and intensity of the external laser field are obtained.

I. Introduction

Interaction of noble gas atoms with strong laser pulses has become an important area of research work for both experimentalists[1,2] and theoreticians[3−10] mainly because of the generation of the higher-order harmonics[11,12] in this process as well as exotic phenomenon like chaotic ionization of He in a microwave field.[13] It is also important to know that how the atom would respond to the external field so far as its reactivity is concerned. Electronegativity[14] (χ) and hardness[15] (η) are two cardinal indices of chemical reactivity. Pauling[16] introduced the concept of electronegativity as the power of an atom in a molecule to attract electrons to itself. The concept of hardness was given by Pearson[17] in his hard−soft acid−base (HSAB) principle which states that, “hard likes hard and soft likes soft”. These popular qualitative chemical reactivity concepts could have been quantified in density functional theory[18] (DFT). The quantitative definitions for electronegativity[19] and hardness[20] for an N-electron system with total energy E can respectively be given as

$$\chi = -\mu = -\left(\frac{\partial E}{\partial N}\right)_{\upsilon(\vec{r}\,)} \tag{1}$$

and

$$\eta = \frac{1}{2}\left(\frac{\partial^2 E}{\partial N^2}\right)_{\upsilon(\vec{r})} = \frac{1}{2}\left(\frac{\partial \mu}{\partial N}\right)_{\upsilon(\vec{r})} \tag{2}$$

In eqs 1 and 2 μ and $\upsilon(\vec{r})$ are chemical potential (Lagrange multiplier associated with the normalization constraint of DFT[17,18]) and external potential, respectively. An equivalent expression[21] for hardness is

$$\eta = \frac{1}{N}\int\int \eta(\vec{r},\vec{r}\,')\, f(\vec{r}\,')\, \rho(\vec{r})\, \mathrm{d}\vec{r}\, \mathrm{d}\vec{r}\,' \tag{3}$$

where $f(\vec{r})$ is the Fukui function[22] and $\eta(\vec{r},\vec{r}\,')$ is the hardness kernel given by[21]

$$\eta(\vec{r},\vec{r}\,') = \frac{1}{2}\, \frac{\delta^2 F[\rho]}{\delta\rho(\vec{r})\, \delta\rho(\vec{r}\,')} \tag{4}$$

where $F[\rho]$ is the Hohenberg−Kohn universal functional of DFT.[18]

The complete characterization of an N-particle system acted on by an external potential $\upsilon(\vec{r})$ requires only N and $\upsilon(\vec{r})$. The response of the system subjected to a change in N at fixed $\upsilon(\vec{r})$ is given by χ and η while the linear response function[17] measures the response of the system when $\upsilon(\vec{r})$ is varied at constant N. If the system is kept under the influence of a weak electric field, polarizability (α) takes care of the corresponding response. A Shannon-type entropy (S) was introduced by Deb and Chattaraj[23] within a quantum fluid density functional framework. During molecule formation the electronegativities of the pertinent atoms get equalized.[24,25] A stable configuration or a favorable process is generally associated with maximum hardness,[26,27] minimum polarizability[28−31] and maximum entropy[32] values. The conditions for maximum hardness and entropy and minimum polarizability complement the usual minimum energy criterion for stability.

Recently Parr et al.[33] have defined the electrophilicity index (W) as

$$W = \frac{\mu^2}{2\eta} \tag{5}$$

We also study here the behavior of ($1/W$), a valid candidate for the nucleophilicity index. Note that the quantity ($1 - W$) will also serve the purpose of a nucleophilicity index. It has also been shown recently[34] that the uncertainty product or the phase space volume (V_{ps}) is a measure of quantum fluctuations and hence has a bearing in the studies of quantum domain behavior of classically chaotic systems.

It has been already demonstrated[35] that in case we focus our attention to a specific atom/molecule taking part in a chemical reaction the whole procedure can be simulated by the interaction

---

* Author for correspondence. E-mail address: pkc@chem.iitkgp.ernet.in.

10.1021/jp0019660 CCC: $20.00

of an atom/molecule with an external field of the strength of the order of the “chemical reaction field”. A molecular reaction dynamics can be envisaged[28] by monitoring the time evolution of the electronegativity of a specific atom from its isolated atom value to the equalized molecular electronegativity value as well as by studying the dynamic profiles of hardness and entropy and how they get maximized and that of the minimization of polarizability during the course of the chemical reaction. In the present work we study the interaction of a He atom in its ground electronic state and an excited electronic state with laser fields of different colors and intensities. The effect of the frequency and the field strength of the external laser field on the overall reactivity of the atom in its various electronic states vis-a-vis the validity of the associated electronic structure principles in a dynamical context as well as the intensities of the generated higher − order harmonics would be understood in this study. The theoretical background of the present work is provided in section II. Section III contains the numerical details, and the results and discussions are given in section IV. Finally, section V presents some concluding remarks.

II. Theoretical Background

Time dependent density functional theory[36] (TDDFT) asserts the unique invertibility of the mapping between the time dependent external potential $\upsilon(\vec{r},t)$ and the density $\rho(\vec{r},t)$. Therefore, all dynamical properties of the system are functionals of $\rho(\vec{r},t)$ and current density $\vec{j}(\vec{r},t)$. To know $\rho(\vec{r},t)$ and $\vec{j}(\vec{r},t)$ of a dynamical system at all times, a quantum fluid density functional theory[23] (QFDFT) was formulated through an amalgamation of TDDFT[36] and quantum fluid dynamics.[37,38] The overall dynamics is studied by solving the following generalized nonlinear Schrödinger equation[23] (GNLSE):

$$\left[-\frac{1}{2}\nabla^2 + \upsilon_{\mathrm{eff}}(\vec{r},t)\right]\phi(\vec{r},t) = i\frac{\partial\phi(\vec{r},t)}{\partial t} \qquad i=\sqrt{-1} \tag{6a}$$

with

$$\phi(\vec{r},t) = \rho^{1/2}\exp(i\xi) \tag{6b}$$

and

$$\vec{j}(\vec{r},t) = [\phi_{re}\nabla\phi_{\mathrm{im}} - \phi_{\mathrm{im}}\nabla\phi_{\mathrm{re}}] = \rho\nabla\xi \tag{6c}$$

where ξ is the velocity potential.

Atomic units are used throughout this paper unless otherwise specified. In the present work we solve this equation to study the temporal evolution of various dynamical quantities including chemical reactivity parameters associated with the interactions of external laser fields of different colors and intensities with a He atom in its ground and excited electronic states. The effective potential of eq 6a is given by

$$\upsilon_{\mathrm{eff}}(\vec{r},t) = \frac{\delta T_{\mathrm{NW}}}{\delta\rho} + \frac{\delta E_{\mathrm{xc}}}{\delta\rho} + \int\frac{\rho(\vec{r},t)}{|\vec{r}-\vec{r}\,'|}\,\mathrm{d}\vec{r}\,' + \upsilon_{\mathrm{ext}}(\vec{r},t) \tag{7}$$

where T_{NW} and E_{xc} denote the non-Weizsäcker part of the kinetic energy and exchange-correlation energy functionals, respectively. It may be noted that this treatment is general and may be applied to systems (atoms and molecules) with more than two electrons as well. However, for a complete treatment, vibrational and rotational degrees of freedom in addition to electronic one are to be considered in the case of molecules.

The kinetic energy functional for this problem is taken as[30]

$$T[\rho] = \frac{1}{8}\int\frac{\nabla\rho\cdot\nabla\rho}{\rho}\,\mathrm{d}\vec{r} + C_k\int\rho^{5/3}\,\mathrm{d}\vec{r} - a(N)\lambda\int\frac{\rho^{4/3}/r}{1+\dfrac{r\rho^{1/3}}{0.043}}\,\mathrm{d}\vec{r} \tag{8a}$$

$$C_k = \left(\frac{3}{10}\right)(3\pi^2)^{2/3}; \qquad \lambda = 30\left(\frac{3}{\pi}\right)^{1/3} \tag{8b}$$

$$a(N) = a_0 + a_1N^{-1/3} + a_2N^{-2/3}$$
$$a_0 = 0.1279, \qquad a_1 = 0.1811, \qquad a_2 = -0.0819 \tag{8c}$$

In eq 8a the first term is the Weizsäcker term and the rest constitutes T_{NW}. This kinetic energy functional is one of the best known functionals as it possesses[30] excellent local and global behavior as well as an acceptable functional derivative. The presence of the Weizsäcker term is also known to be important.[39]

The explicit form for E_{xc} is taken as

$$E_{\mathrm{xc}}[\rho] = E_{\mathrm{x}}[\rho] + E_{\mathrm{c}}[\rho] \tag{9a}$$

where $E_{\mathrm{x}}[\rho]$ is the Dirac exchange functional modified in the spirit of Becke’s functional,[40] as follows[41]

$$E_{\mathrm{x}}[\rho] = -C_{\mathrm{x}}\left[\int\rho^{4/3}\,\mathrm{d}\vec{r} + \int\frac{\rho^{4/3}}{1+(r^2\rho^{2/3}/0.0244)}\,\mathrm{d}\vec{r}\right]; \qquad C_{\mathrm{x}} = \left(\frac{3}{4\pi}\right)(3\pi^2)^{1/3} \tag{9b}$$

and $E_{\mathrm{c}}[\rho]$ is a Wigner-type parametrized correlation energy functional given by[42]

$$E_{\mathrm{c}}[\rho] = -\int\frac{\rho}{9.81 + 21.437\rho^{-1/3}}\,\mathrm{d}\vec{r} \tag{9c}$$

The external TD potential for the present problem of He atom interacting with a laser field linearly polarized in z-direction may be written as

$$\upsilon_{\mathrm{ext}}(\vec{r},t) = -\frac{2}{r} + \epsilon 1\, z, \quad \text{for a monochromatic pulse} \tag{10a}$$

$$= -\frac{2}{r} + \epsilon 2\, z, \quad \text{for a bichromatic pulse} \tag{10b}$$

where

$$\epsilon 1 = \epsilon\sin(\omega_0 t) \tag{10c}$$

and

$$\epsilon 2 = 0.5\epsilon[\sin(\omega_0 t) + \sin(\omega_1 t)] \tag{10d}$$

To have slow oscillations during and after the laser source being switched on, ϵ is written in terms of the maximum amplitude ϵ_0 and the switch-on time t' as

$$\epsilon = \epsilon_0 t/t' \qquad \text{for} \qquad 0 \le t \le t' \tag{10e}$$

$$= \epsilon_0 \qquad \text{otherwise} \tag{10f}$$

For the present problem a time dependent energy quantity, $E(t)$ can be defined[36−38] as the following density functional

$$E(t) = \frac{1}{2}\int \rho(\vec{r},t)|\nabla\xi|^2 \, d\vec{r} + T[\rho] + E_{xc}[\rho] + \frac{1}{2}\int\int \frac{\rho(\vec{r},t)\,\rho(\vec{r}\,',t)}{|\vec{r} - \vec{r}\,'|} \, d\vec{r} \, d\vec{r}\,' + \int v_{ext}(\vec{r},t)\,\rho(\vec{r},t)\, d\vec{r} \quad (11)$$

where the first term represents the macroscopic kinetic energy which vanishes for a state with zero current density, for example in the ground state of a system. A similar time dependent total energy functional has been used before by other workers.[38] The associated chemical potential may be defined as

$$\mu(t) = \frac{\delta E(t)}{\delta\rho} = \frac{1}{2}|\nabla\xi|^2 + \frac{\delta T}{\delta\rho} + \frac{\delta E_{xc}}{\delta\rho} + \int \frac{\rho(\vec{r}\,',t)}{|\vec{r} - \vec{r}\,'|} \, d\vec{r}\,' + v_{ext}(\vec{r},t) \quad (12)$$

Now as a TD extension to Gordy's work[43] the TD chemical potential becomes equal to the total electrostatic potential at a point $\vec{r}_c$ (cf. eq 12), viz.,

$$-\chi(t) = \mu(t) = \int \frac{\rho(\vec{r},t)}{|\vec{r}_c - \vec{r}|} \, d\vec{r} + v_{ext}(\vec{r}_c,t) \quad (13a)$$

where r_c is the point where the sum of functional derivatives of total kinetic energy and exchange-correlation energy is zero, i.e.,

$$\frac{1}{2}|\nabla\xi|^2 + \frac{\delta T}{\delta\rho} + \frac{\delta E_{xc}}{\delta\rho} = 0 \quad (13b)$$

It may be noted that the condition 13b at $t = 0$ is equivalent to that of the ground-state DFT[18] since $\vec{j}(\vec{r},0) = 0$. Politzer et al. [44] had shown through the application of the electronegativity equalization principle that r_c values provide very good estimates of the covalent radii of the atoms.

To follow the hardness dynamics using eq 3, the Fukui function is modeled as follows[22]

$$f(\vec{r}) = \frac{s(\vec{r})}{\int s(\vec{r})\, d\vec{r}} \quad (14a)$$

where the local softness $s(\vec{r})$ is taken as[45]

$$s(\vec{r}) = \frac{\delta(\vec{r} - \vec{r}\,')}{2\eta(\vec{r},\vec{r}\,')} \quad (14b)$$

The hardness kernel $\eta(\vec{r},\vec{r}\,')$ (eq 4) is calculated using the following local form[30] for $F[\rho]$

$$F[\rho] = T^{local}[\rho] + V_{ee}^{\ local}[\rho] \quad (14c)$$

where the local kinetic energy[41] and electron−electron repulsion energy[46] are taken as

$$T^{local}[\rho] = C_k\int \rho^{5/3} \, d\vec{r} + C_x\int \frac{\rho^{4/3}/r}{1 + \frac{r\rho^{1/3}}{0.043}} \, d\vec{r} \quad (14d)$$

and

$$V_{ee}^{\ local}[\rho] = 0.7937(N - 1)^{2/3}\int \rho^{4/3} \, d\vec{r} \quad (14e)$$

These local functionals are used because of the simplicity in the calculation of the second-order functional derivative (eq 4) and the associated Fukui function within this local model[42]

The dynamic polarizability is written as

$$\alpha(t) = |D_{ind}^{\ z}(t)|/|F_z(t)| \quad (15a)$$

where $D_{ind}^{\ z}(t)$ is the electronic part of the induced dipole moment given as

$$D_{ind}^{\ z}(t) = \int z\rho(\vec{r},t)\, d\vec{r} \quad (15b)$$

and $F_z(t)$ is the z-component of the external field.

The TD entropy is defined as[23]

$$S(t) = \int \left\{\frac{5}{2} - \ln \rho(\vec{r},t) + \frac{3}{2}\ln(k\theta(\vec{r},t)/2\pi)\right\} k\rho(\vec{r},t)\, d\vec{r} \quad (16a)$$

where k is the Boltzmann constant and $\theta(\vec{r},t)$ is a space−time dependent temperature given in terms of the kinetic energy density $t_s(\vec{r},\rho(\vec{r},t))$ as[23]

$$t_s(\vec{r};\rho(\vec{r},t)) = \frac{3}{2}k\theta(\vec{r},t)\,\rho(\vec{r},t) + \left[\frac{|\vec{j}(\vec{r},t)|^2}{2\rho(\vec{r},t)}\right] \quad (16b)$$

The phase space volume or the uncertainty product, V_{ps} has been shown[34,47] to be an important diagnostic of the quantum signature of classical chaos[47] as related to the compactness of the electron cloud.[48] For the present problem it may be defined as

$$V_{ps} = \{\langle(p_{\tilde{\rho}} - \langle p_{\tilde{\rho}}\rangle)^2\rangle\langle(p_z - \langle p_z\rangle)^2\rangle\langle(\tilde{\rho} - \langle\tilde{\rho}\rangle)^2\rangle\langle(z - \langle z\rangle)^2\rangle\}^{1/2} \quad (17)$$

A sharp increase in $V_{ps}(t)$ signals a chaotic motion[47] since it is a measure of the associated quantum fluctuations.[47]

To generate the harmonic spectrum, the induced dipole moment, $D_{ind}^{\ z}(t)$ is Fourier transformed to obtained $d(\omega)$. It has been shown[49] that the absolute square of the Fourier transform, $|d(\omega)|^2$ is roughly proportional to the experimental harmonic distribution.

III. Numerical Solution

Since the electron density varies rapidly near the nucleus and relatively slowly elsewhere the variables are transformed as follows

$$y = \tilde{\rho}\phi \quad (18a)$$

and

$$\tilde{\rho} = x^2 \quad (18b)$$

where $\tilde{\rho}$ is one of the cylindrical polar coordinates $(\tilde{\rho},\tilde{\phi},z)$. The azimuthal symmetry of the physical system allows us to analytically integrate over $0 \le \tilde{\phi} \le 2\pi$. The GNLSE (eq 6a) takes the following form in the transformed variables after the $\tilde{\phi}$ integration,

$$\left\{\left(\frac{3}{4x^3}\right)\frac{\partial y}{\partial x} - \left(\frac{1}{4x^2}\right)\frac{\partial^2 y}{\partial x^2} - \frac{\partial^2 y}{\partial z^2}\right\} - \left(\frac{1}{x^4} - 2v_{eff}\right)y = 2i\,\frac{\partial y}{\partial t} \quad (19)$$

A leapfrog-type finite difference scheme has been adopted to numerically solve the eq 19 as an initial boundary value problem. An alternating direction implicit (ADI) method is employed to generate the density at the second time step from

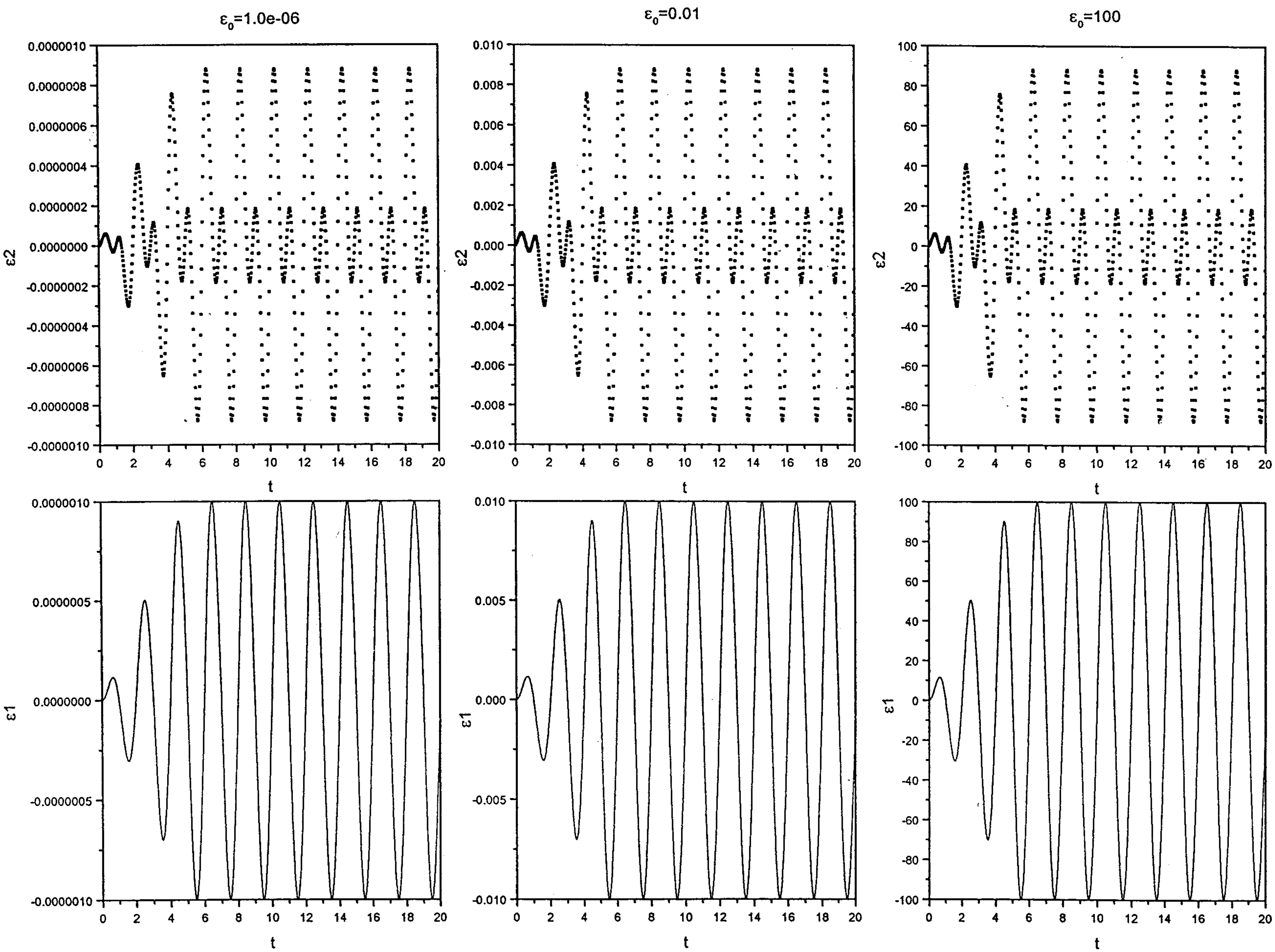

Figure 1. Time evolution of the external electric field: $\epsilon 1$ (—) monochromatic pulse; $\epsilon 2$ (···) bichromatic pulse. Maximum amplitudes: $\epsilon_0 = 10^{-6}$, 0.01, 100; $\omega_0 = \pi$, $\omega_1 = 2\omega_0$.

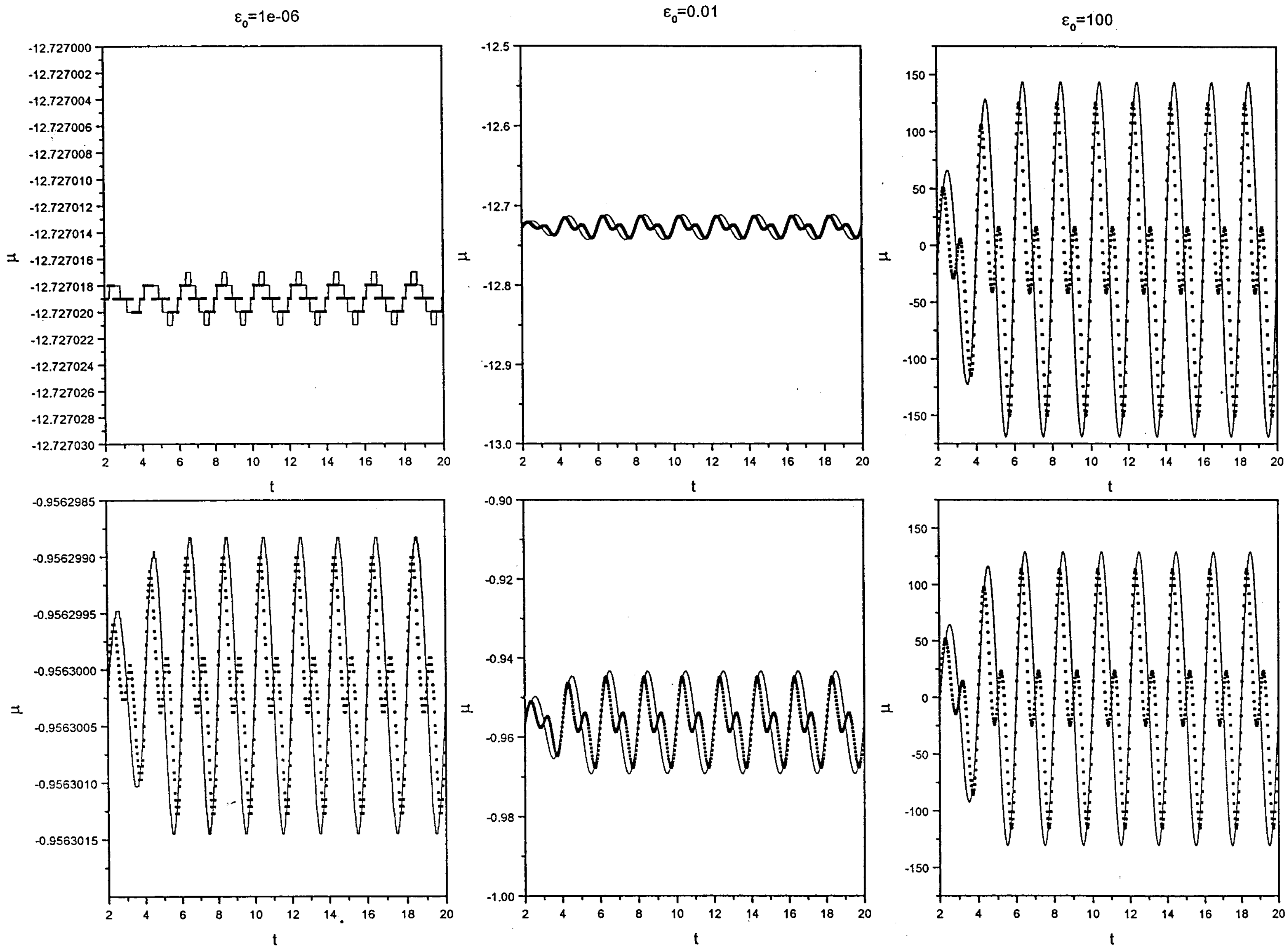

Figure 2. Time evolution of Chemical potential (μ) when a helium atom is subjected to external electric fields (GS, ground state; ES, excited state): (—) monochromatic pulse; (···) bichromatic pulse. Maximum amplitudes: $\epsilon_0 = 10^{-6}$, 0.01, 100; $\omega_0 = \pi$, $\omega_1 = 2\omega_0$.

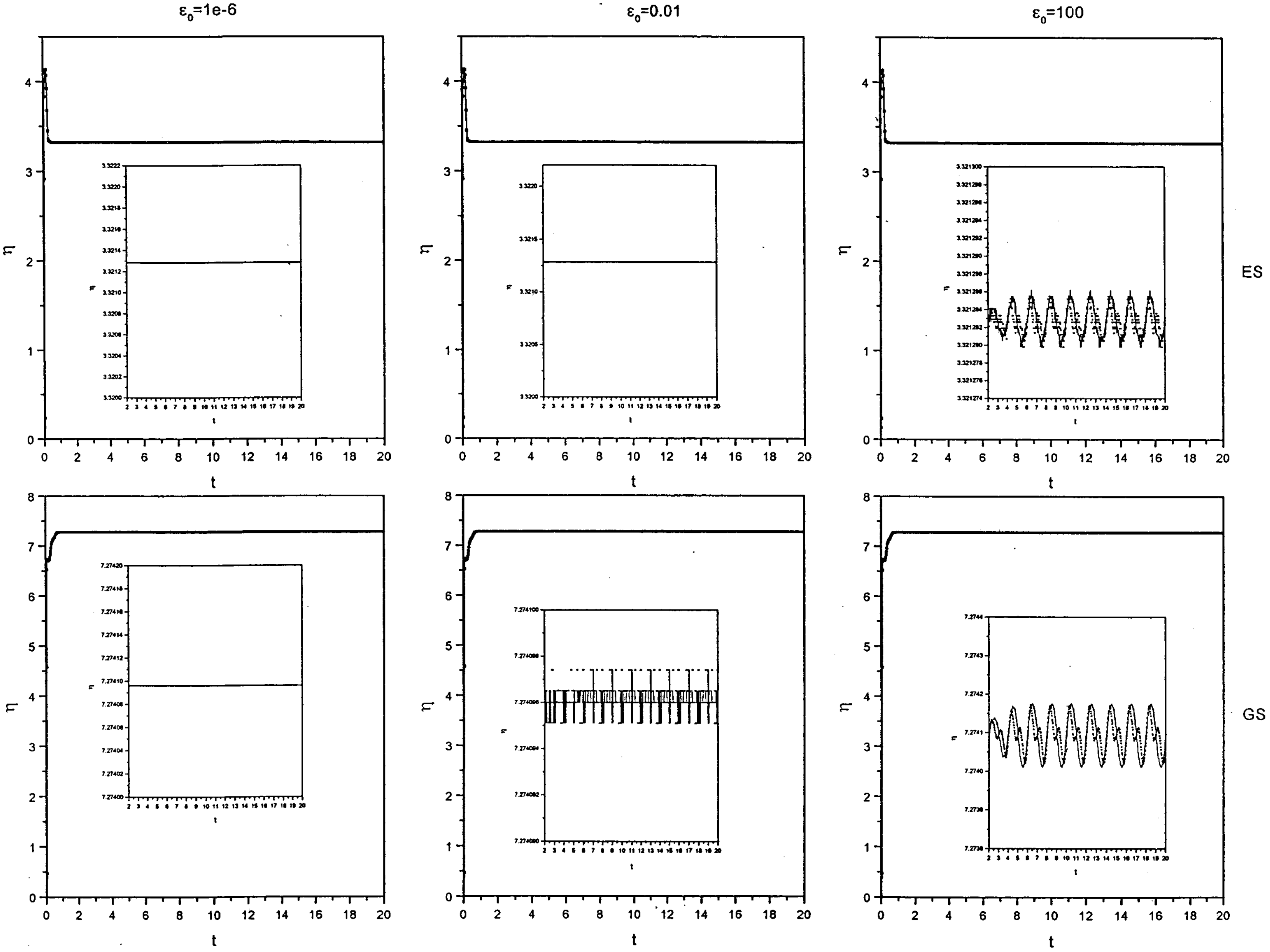

Figure 3. Time evolution of hardness (η) when a helium atom is subjected to external electric fields (GS, ground state; ES, excited state): (—) monochromatic pulse; (···) bichromatic pulse. Maximum amplitudes: $\epsilon_0 = 10^{-6}$, 0.01, 100; $\omega_0 = \pi$, $\omega_1 = 2\omega_0$.

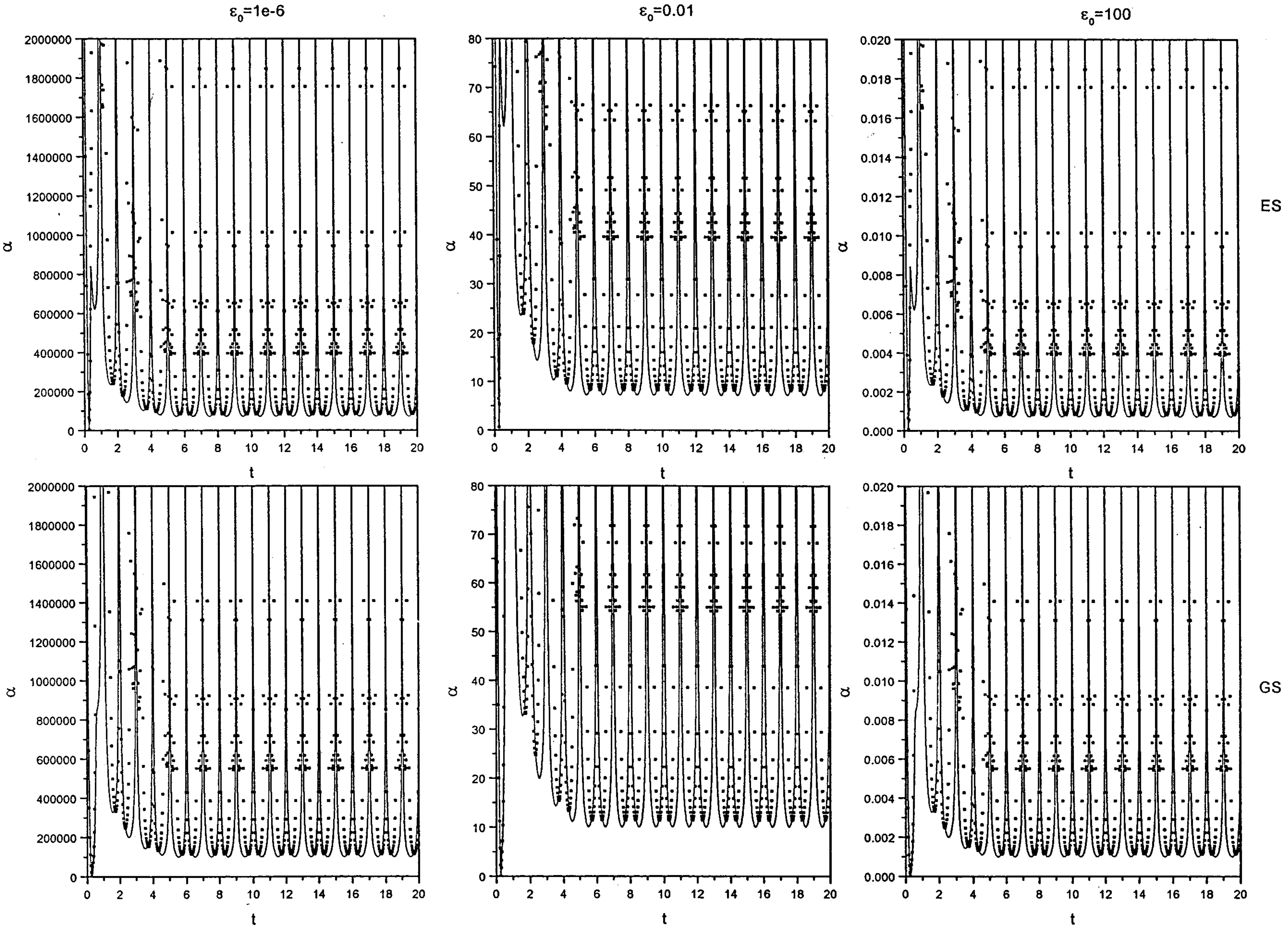

Figure 4. Time evolution of polarizability (α) when a helium atom is subjected to external electric fields (GS, ground state; ES, excited state): (—) monochromatic pulse; (···) bichromatic pulse. Maximum amplitudes: $\epsilon_0 = 10^{-6}$, 0.01, 100; $\omega_0 = \pi$, $\omega_1 = 2\omega_0$.

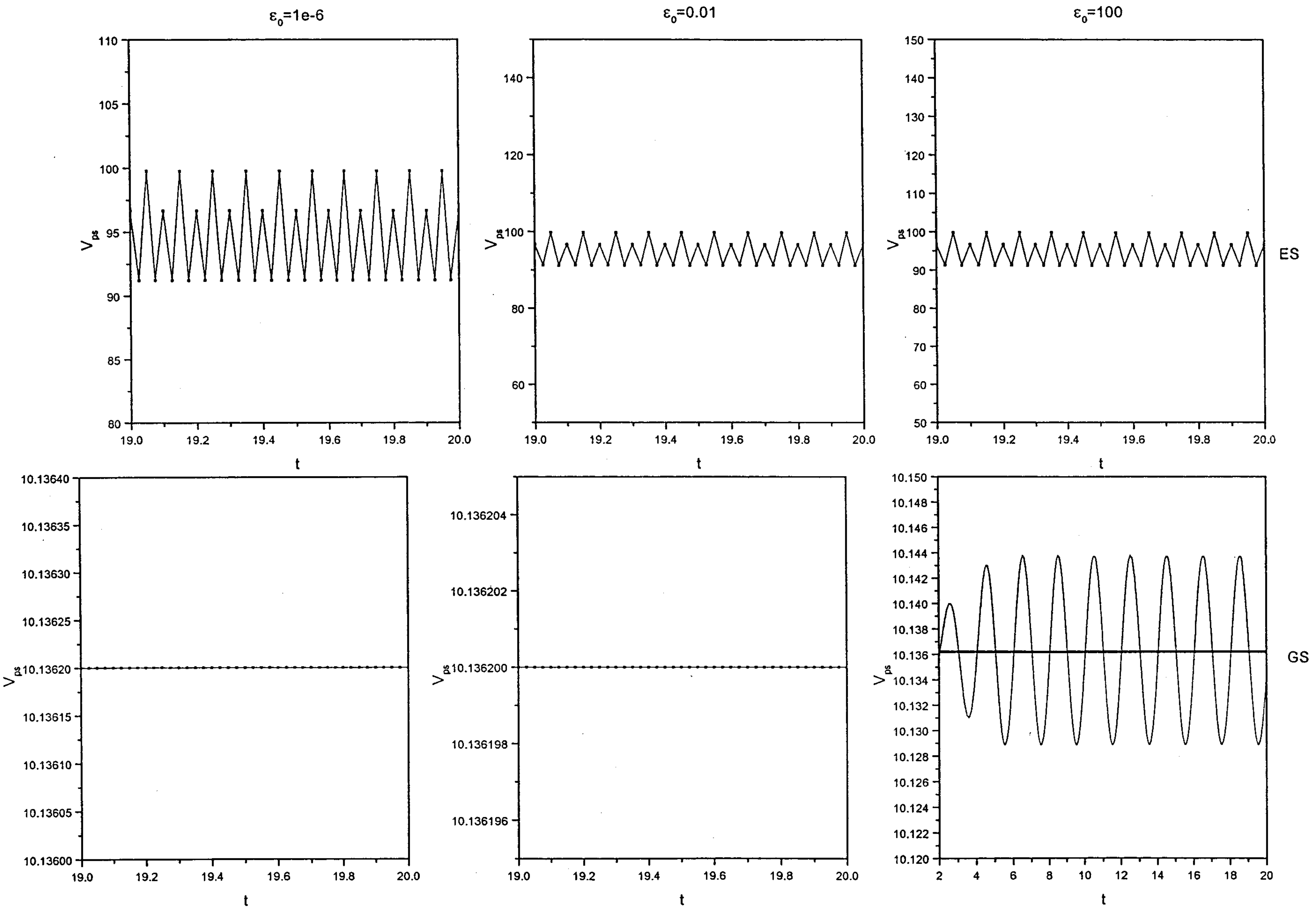

Figure 5. Time evolution of phase volume (V_{ps}) when a helium atom is subjected to external electric fields (GS, ground state; ES, excited state): (—) monochromatic pulse; (···) bichromatic pulse. Maximum amplitudes: $\epsilon_0 = 10^{-6}$, 0.01, 100; $\omega_0 = \pi$, $\omega_1 = 2\omega_0$.

TABLE 1: Calculated Reactivity Indices (au) at $t = 0$ for He Atom in Different Electronic States[a]

electronic state; electronic configuration	χ	η	V_{ps}	S	W	$^1/_W$	α	$\|d(\omega_0)\|^2$
^{1}S; 1s^2	0.2591	0.3920	0.5563×10^2	4.0040	0.0856	11.6822	0.6336×10^3	6.01734
^{1}P; 1s2p	0.2044	0.1315	0.5067×10^5	2.6528	0.1589	6.2933	0.3799×10^4	5.1615

[a] Values of α and $|d(\omega_0)|^2$ are at the time step at the end of one ADI cycle as the He atom interacts with the monochromatic field with $\epsilon_0 = 0.01$.

the input density which is required for the leapfrog scheme to start. A detailed discussion on the derivation of eq 19 and the numerical method for its solution can be found elsewhere.[23,35] To launch the numerical solution, near-Hartree−Fock densities of He atom in the ^{1}S ground state[50] and a ^{1}P excited state of the 1s2p electronic configuration[51] have been employed. The temporal mesh size was taken as $\Delta t = 0.025$ au. Different spatial grid sizes were chosen for the ground and excited-state calculations. For the ground and excited states, we took $\Delta x = \Delta z = 0.05$ au and $\Delta x = \Delta z = 0.036$ au, respectively. Larger domains for x and z were taken when the excited-state density was used.

We choose $t' = 5$, $\omega_0 = \pi$, $\omega_1 = 2\omega_0$ and three different maximum amplitude values $\epsilon_0 = 10^{-6}$, 0.01 and 100, respectively. To our knowledge, the calculation of so many reactivity indices in a time dependent situation for a system in both ground and excited electronic states interacting with external fields of different colors and intensities is done here for the first time.

IV. Results and Discussions

The time evolution of different reactivity parameters are depicted in Figures 1−8. All quantities are in atomic units. Unless otherwise specified, in all the figures, GS and ES refer to the ground and excited states of the helium atom, respectively, and a solid line and scattered points respectively signify monochromatic and bichromatic pulses. Three different field intensities corresponding to $\epsilon_0 = 10^{-6}$, 0.01 and 100 are shown separately.

Figure 1 presents the time dependence of the external field with different frequencies and amplitudes.

Initial values ($t = 0$) of all the reactivity parameters (essentially the corresponding values of the He atom) but for $\alpha(t)$ and $|d(\omega_0)|^2$ (values for these quantities are reported after the end of the ADI cycle since they explicitly depend on the response of the atom when it interacts with the external field) are presented in Table 1. Both electronegativity and hardness values for the ground state are larger than the corresponding excited state values. Since a system is generally more reactive in the excited state it is expected from the maximum hardness principle[26,27] (MHP). Larger V_{ps} value for the excited-state refers to larger quantum fluctuations than in the ground state. Ground-state entropy is larger than the corresponding excited-state value, as expected from the maximum entropy principle[32] (MEP). Helium is comparatively less electrophilic and more nucleophilic in its ground state than in the excited state. The He atom is less polarizable in its ground state than in the excited state as would have been dictated by the minimum polarizability principle[28−31] (MPP). Intensity of the first harmonic is larger in the ground state for the monochromatic pulse with $\epsilon_0 = 0.01$.

Temporal evolution of the chemical potential is depicted in Figure 2. Magnitude of μ is always larger in the excited state. It exhibits characteristic oscillations. But for the initial transients the oscillations in μ is in phase with the external field. Reactivity profiles help in visualizing the overall dynamical process. Only when the field intensity is very low are the oscillations not clearly in phase with the external field. Once the intensity of the external field is increased beautiful in phase oscillations for both the electronic states are shown by the dynamic μ-profile which is a highly satisfactory feature considering the complicated round about way of the calculation of μ. A small portion of this work was published elsewhere.[10] It is important to note that the amplitude of μ-oscillations becomes very large for $\epsilon_0 = 100$ for both the electronic states and for both monochromatic and bichromatic pulses.

Figure 3 presents the time evolution of hardness. After the initial transients η attains a more or less steady value which is larger for the ground state than for the excited state, a signature of MHP. It may be noted that all quantities are not equally sensitive to the external perturbation. Some oscillate in phase, some out of phase and others remain steady. Unlike oscillation in μ, it is observed that η maintains a steady value but for the initial transients. It may be due to the fact that the first-order variation in energy due to external perturbation is significantly larger than the corresponding second-order one. Overall dynamics may be envisaged as follows. The nuclear Coulomb field being central in nature the atomic electron density distribution will have spherical symmetry. Once the external z-polarized laser pulse is switched on there will be a competition between the two to govern the electron density distribution, viz., the latter would try to make it cylindrically symmetric. When the intensity of the external field is very small, it is essentially the atomic density with some amount of pulsation. For an oscillating atom, it may be assumed that those quantities will oscillate in phase which are strongly dependent on the electron density distribution. With an increase in the strength of the external laser field an oscillating dipole will result which would emit radiation including higher order harmonics. In the present work we also study this harmonic spectrum. This dynamical picture is corroborated by the fact that for a weak field even μ-oscillations are not clear-cut in phase with external field because the effect of nuclear Coulomb field is still not overcome by the laser pulse. In Figure 3 we magnify the steady parts of the η-profile and show in respective insets. It is now transparent that for $\epsilon_0 = 10^{-6}$ there is no visible effect of the external field, for $\epsilon_0 = 0.01$ still competition is going on while for $\epsilon_0 = 100$ the dynamics is totally dominated by the external field and the in phase oscillation in the η-profile are clearly manifested for both the electronic states and for both monochromatic and bichromatic laser pulses.

Dynamic polarizability is presented in Figure 4. The frequency of oscillation in α is twice that of the external field. For any extremum in the external field there corresponds to a minimum in α and the latter blows up when the former becomes zero. Here also if we compare the respective minimum α values (α_{min}) for the two electronic states, α_{min} for the ground state is smaller than that of the excited state, which is in conformity with MPP.

Figure 5 shows the phase volume or the uncertainty product, V_{ps}. It confirms that the quantum fluctuations are always larger[47] in the excited state than in the ground state as is also expected from the more compactness of the ground-state electron cloud.[48] For this quantity in phase oscillations are seen only for the ground state of the atom interacting with the monochromatic pulse of $\epsilon_0 = 100$. If the field is not very strong both

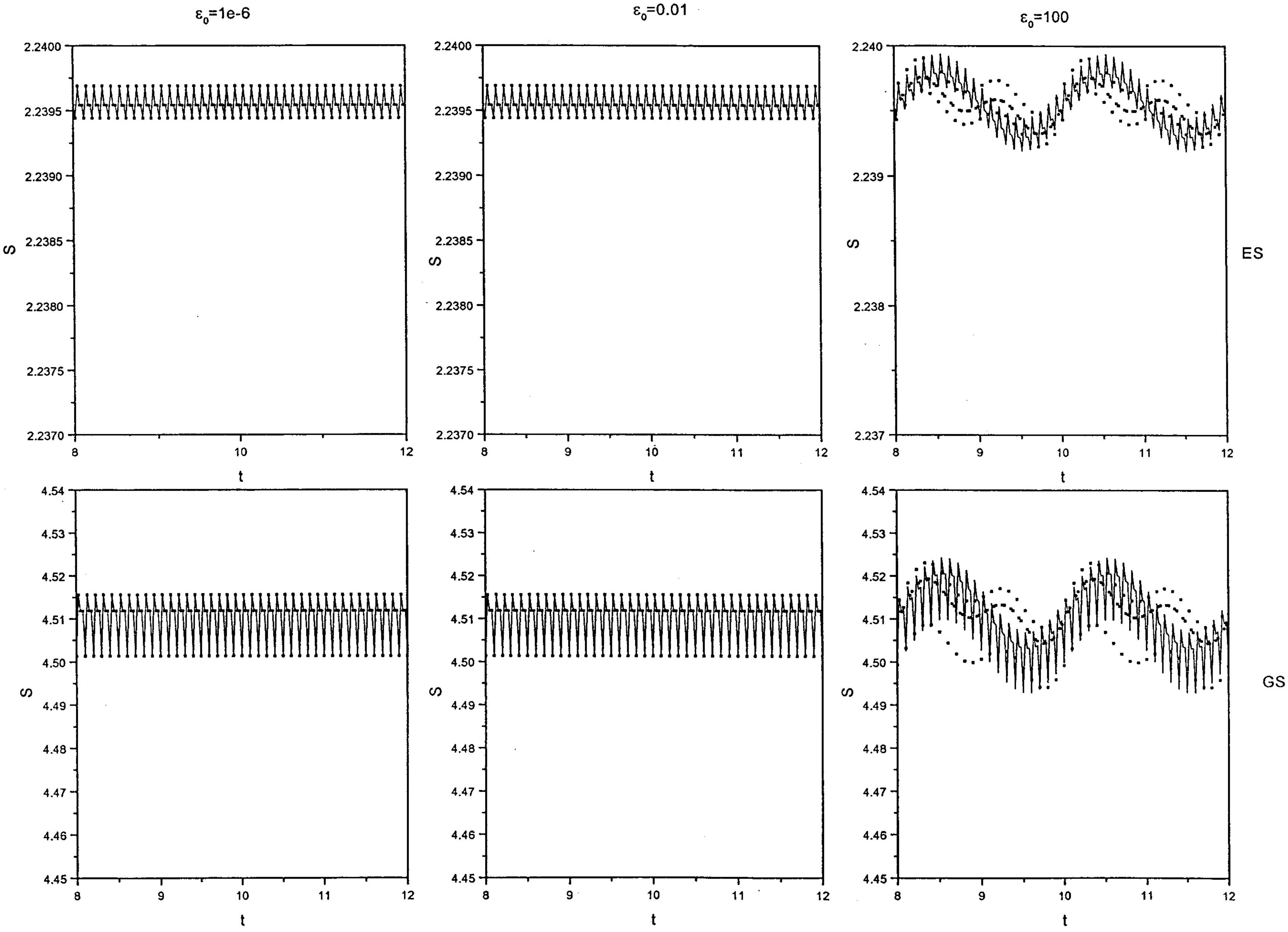

Figure 6. Time evolution of entropy (S) when a helium atom is subjected to external electric fields (GS, ground state; ES, excited state): (—) monochromatic pulse; (···) bichromatic pulse. Maximum amplitudes: $\epsilon_0 = 10^{-6}$, 0.01, 100; $\omega_0 = \pi$, $\omega_1 = 2\omega_0$.

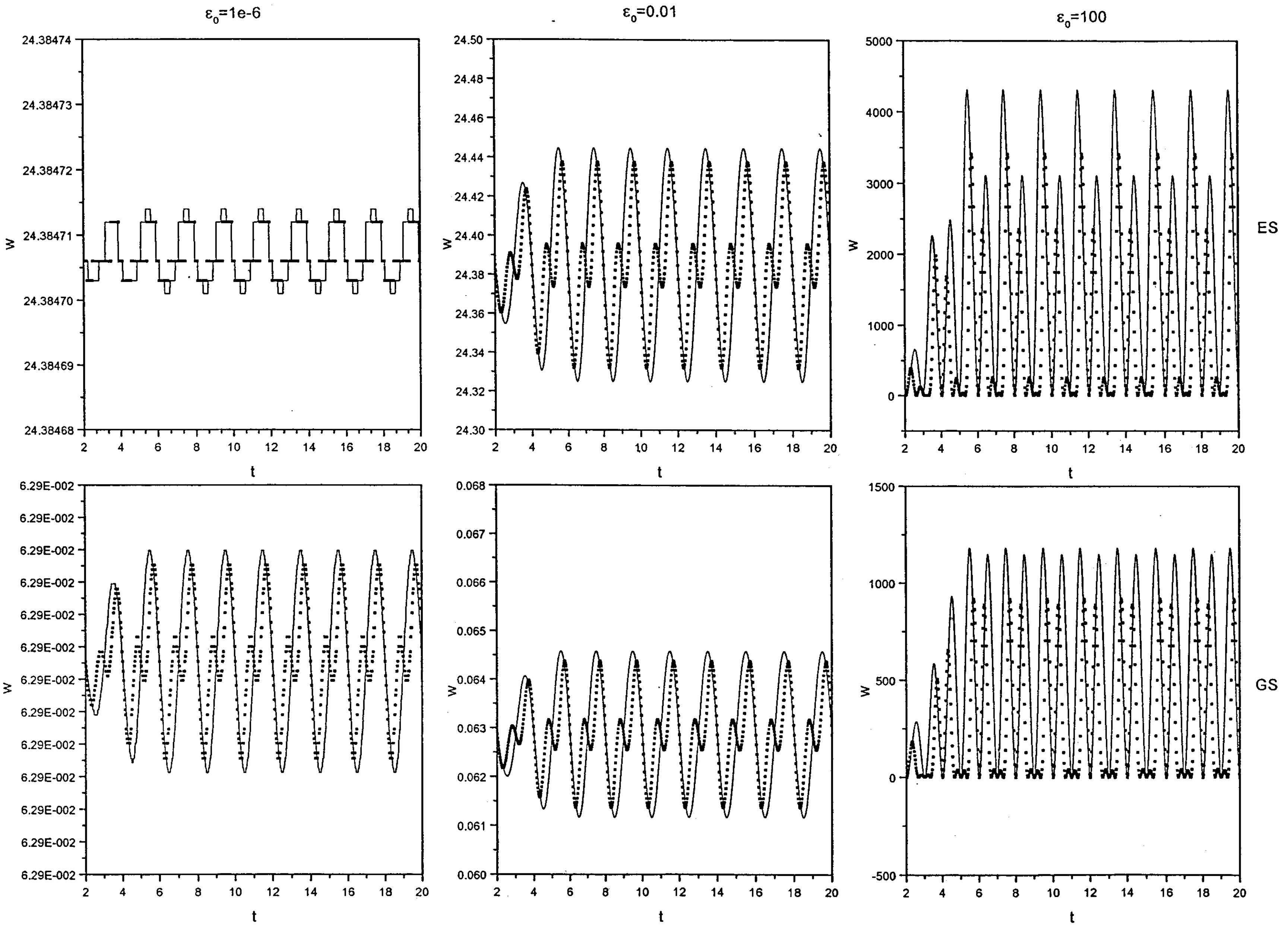

Figure 7. Time evolution of electrophlicity index (*W*) when a helium atom is subjected to external electric fields (GS, ground state; ES, excited state): (—) monochromatic pulse; (···) bichromatic pulse. Maximum amplitudes: $\epsilon_0 = 10^{-6}$, 0.01, 100; $\omega_0 = \pi$, $\omega_1 = 2\omega_0$.

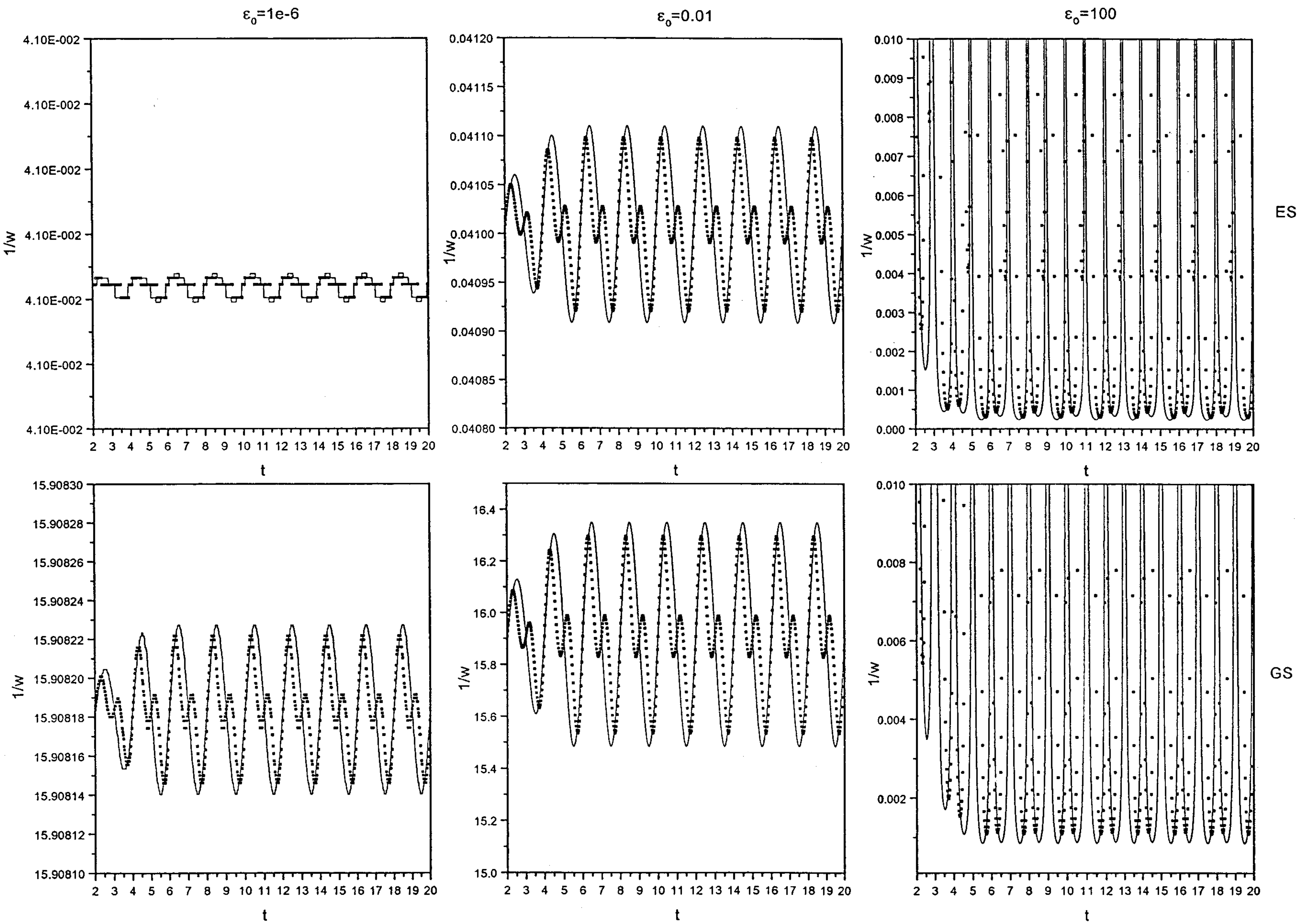

Figure 8. Time evolution of nucleophlicity index ($^1/_w$) when a helium atom is subjected to external electric fields (GS, ground state; ES, excited state): (—) monochromatic pulse; (···) bichromatic pulse. Maximum amplitudes: $\epsilon_0 = 10^{-6}$, 0.01, 100; $\omega_0 = \pi$, $\omega_1 = 2\omega_0$.

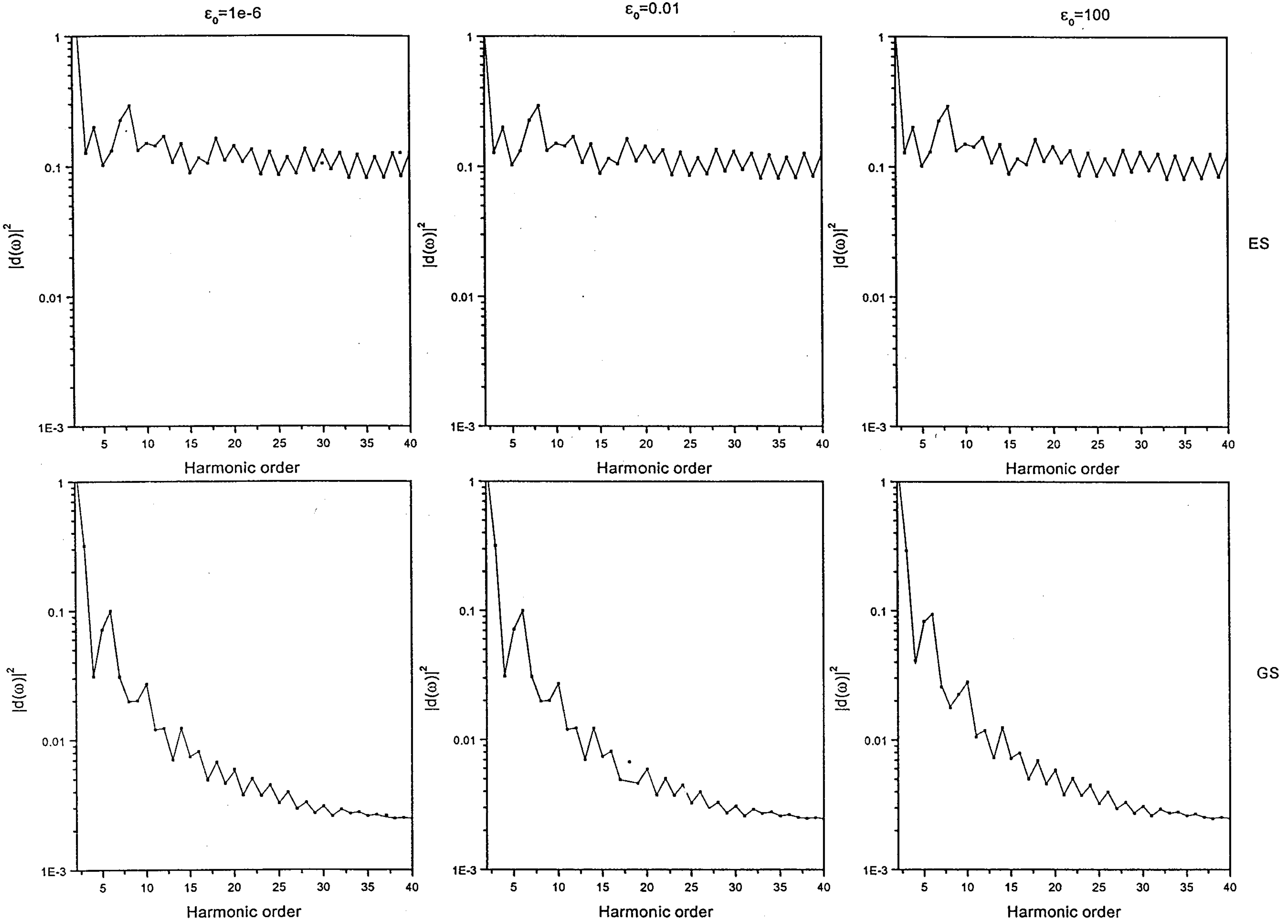

Figure 9. Harmonic spectra of helium atom for various laser frequencies and intensities (GS, ground state; ES, excited state): (—) monochromatic pulse; (···) bichromatic pulse. Maximum amplitudes: $\epsilon_0 = 10^{-6}$, 0.01, 100; $\omega_0 = \pi$, $\omega_1 = 2\omega_0$.

monochromatic and bichromatic pulses behave more or less similarly. Excited states always show oscillations when compared with the corresponding ground state V_{ps} profiles.

Time evolution of entropy is given in Figure 6. It exhibits rapid periodic oscillations after initial transients die out. As expected from MEP the amplitude of S for the ground-state is always larger than that for the excited state. When the field strength is not very strong ($\epsilon_0 = 10^{-6}$, 0.01), this behavior is due to nonlinear charge oscillations from a pulsating atom where the effect of the external field is not dominating as is confirmed by the fact that both monochromatic and bichromatic pulses exhibit similar oscillations. For a very intense field ($\epsilon_0 = 100$) these oscillations persist with the corresponding envelope showing the beautiful in phase oscillations distinctly different for monochromatic and bichromatic pulses.

Figures 7 and 8 depict respectively the dynamic profiles of electrophilicity and nucleophilicity indices respectively. For $\epsilon_0 = 10^{-6}$ both W and $1/W$ show in phase oscillations for the ground state while the excited state shows oscillations characteristic of the resultant field of two competing ones. Both the electronic states show in phase oscillations for $\epsilon_0 = 0.01$. However, for $\epsilon_0 = 100$ oscillations appear somewhat different, especially the $1/W$ plots resemble the corresponding α plots.

An analysis of the dynamical profiles of chemical potential, hardness and electrophilicity reveals that a low intensity field is sufficient to cause in-phase oscillations in the case of the chemical potential and electrophilicity but for a similar effect in the case of the hardness a stronger field is necessary. Profiles of chemical potential and electrophilicity are supposed to exhibit a mirror image relationship since electronegativity and electrophilicity must follow similar trends. In the present calculation we found this to be true but for the case of very large intensity of the external field which may be due to oscillation in hardness along with that of chemical potential at that intensity. It is expected that a different choice of the functionals for kinetic, exchange and correlation energies would produce different numerical values of these reactivity indices. However, the qualitative features of the respective dynamical profiles will be similar.

Finally, the harmonic spectra are presented in Figure 9. Envelopes of these plots look like those reported by Erhard and Gross.[6] We found that the harmonics generated by the bichromatic pulse is generally more intense than those resulted from the monochromatic one albeit not by one or two orders of magnitude as shown before[6] and accordingly not discernible in the scale of the plot. Harmonic spectrum levels off for lower harmonic order for the ground state than that for the excited state.

V. Concluding Remarks

A quantum fluid density functional approach is adopted to study the dynamics of a helium atom in its ground and excited electronic states interacting with z-polarized laser pulses of different colors and intensities. Dynamical variants of the principles of electronegativity equalization, maximum hardness, minimum polarizability and maximum entropy manifest themselves. A tug-of-war between the spherically symmetric nuclear Coulomb field and cylindrically symmetric external electric field to govern the electron density distribution is clearly delineated through the dynamical profiles of various reactivity indices like electronegativity, hardness, polarizability, entropy, electrophilicity and nucleophilicity indices and phase volume for the external field of varying strengths. Harmonic spectra of the higher order harmonics included in the radiation emitted by the resulting oscillating dipole have been analyzed.

Acknowledgment. We thank CSIR, New Delhi, for financial support and Dr. S. Sengupta for his help in various ways. P.K.C. is grateful to Professor E. K. U. Gross for his kind interest. This paper forms a part of the invited talk delivered by P.K.C. in the DFT2000 satellite symposium of the 10th International Congress of Quantum Chemistry held in Menton, France. P.K.C. gratefully acknowledges the partial financial assistance toward attending this symposium, from INSA and CSIR, New Delhi and IIT Kharagpur.

References and Notes

(1) L'Huillier, A.; Balcou, P. *Phys. Rev. Lett.* **1993**, *70*, 774.

(2) Preston, S. G.; Sanpera, A.; Zepf, M.; Blyth, W. J.; Smith, C. G.; Wark, J. S.; Key, M. H.; Burnett, K.; Nakai, M.; Neely, D.; Offenberger, A. A. *Phys. Rev. A* **1996**, *53*, R31.

(3) Sanpera, A.; Jönsson, P.; Watson, J. B.; Burnett, K. *Phys. Rev. A* **1995**, *51*, 3148.

(4) Chen, X.; Sanpera, A.; Burnett, K. *Phys. Rev. A* **1995**, *51*, 4824.

(5) Watson, J. B.; Sanpera, A.; Burnett, K. *Phys. Rev. A* **1995**, *51*, 1458.

(6) Erhard, S.; Gross, E. K. U. In *Multiphoton Processes 1996*; Lambropoulos, P., Walther, H., Eds.; IOP Publishing: London, 1997; pp 37−45 and references therein.

(7) Ullrich, C. A.; Gross, E. K. U. *Comments At. Mol. Phys.* **1997**, *33*, 211 and references therein.

(8) Chattaraj, P. K. *Int. J. Quantum Chem.* **1992**, *41*, 845.

(9) Dey, B. K.; Deb, B. M. *Int. J. Quantum. Chem.* **1995**, *56*, 707.

(10) Chattaraj, P. K.; Sengupta, S.; Poddar, A. *Int. J. Quantum Chem.* **1998**, *69*, 279.

(11) McPherson, A.; Gibson, G.; Jara, H.; Johann, U.; Luk, T. S.; McIntyre, I. A.; Boyer, K.; Rhodes, C. K. *J. Opt. Soc. Am.* **1987**, *B4*, 595.

(12) (a) *Atoms in Intense Laser Fields*; Gavrila, M., Ed.; Academic Press: Boston, 1992. (b) *Super-Intense Laser—Atom Physics*; Piraux, B., L'Huillier, A., Rzazewski, K., Eds.; NATO ASI Series B316; Plenum Press: New York, 1993.

(13) Mariani, D. R.; Van de Water, W.; Koch, P. M.; Bergeman, T. *Phys. Rev. Lett.* **1983**, *50*, 1261. Van de Water, W.; Yoakum, S.; Van Leeuwen, K. A. H.; Sauer, B. E.; Moorman, L.; Galvez, E. J.; Mariani, D. R.; Koch, P. M. *Phys. Rev. A* **1990**, *42*, 573. Sanders, M. M.; Jensen, R. V. *Am. J. Phys.* **1996**, *64*, 1013.

(14) *Electronegativity: Struct. Bonding;* Sen, K. D., Jorgenson. C. K., Eds.; Springer-Verlag: Berlin, 1987; Vol. 66.

(15) *Chemical Hardness: Struct. Bonding*; Sen, K. D., Mingos, D. M. P., Eds.; Springer-Verlag: Berlin, 1993; Vol. 80.

(16) Pauling, L. *The Nature of the Chemical Bond*, 3rd ed.; Cornell University Press: Ithaca, NY, 1960.

(17) Pearson, R. G. *Coord. Chem. Rev.* **1990**, *100*, 403; *Hard and Soft Acids and Bases*; Dowden, Hutchinson and Ross: Stroudsberg, PA, 1973.

(18) Hohenberg, P.; Kohn, W. *Phys. Rev. B* **1964**, *136*, 864. Kohn, W.; Sham, L. J. *J. Phys. Rev. A* **1965**, *140*, 1133. Parr, R. G.; Yang, W. *Density Functional Theory of Atoms and Molecules*; Oxford University Press: Oxford, 1989; *Annu. Rev. Phys. Chem.* **1995**, *46*, 701. Chattaraj, P. K. *J. Indian. Chem. Soc.* **1992**, *69*, 173. Kohn, W.; Becke, A. D.; Parr, R. G. *J. Phys. Chem.* **1996**, *100*, 12974.

(19) Parr, R. G.; Donelly, D. A.; Levy, M.; Palke, W. E. *J. Chem. Phys.* **1978**, *68*, 3801.

(20) Parr, R. G.; Pearson, R. G. *J. Am. Chem. Soc.* **1983**, *105*, 7512.

(21) Berkowitz, M.; Ghosh, S. K.; Parr, R. G. *J. Am. Chem. Soc.* **1985**, *107*, 6811. Ghosh, S. K.; Berkowitz, M. *J. Chem. Phys.* **1985**, *83*, 2976.

(22) Parr, R. G.; Yang, W. *J. Am. Chem. Soc.* **1984**, *106*, 4049.

(23) Deb, B. M.; Chattaraj, P. K. *Phys. Rev. A* **1989**, *39*, 1696.

(24) Sanderson, R. T. *Science* **1951**, *114*, 670; *Science* **1955**, *121*, 207; *J. Chem. Educ.* **1954**, *31*, 238.

(25) Politzer, P.; Weinstein, H. *J. Chem. Phys.* **1979**, *70*, 3680. Parr, R. G.; Bartolotti, L. J. *J. Am. Chem. Soc.* **1982**, *104*, 3081. Nalewajski, R. F. *J. Phys. Chem.* **1985**, *89*, 2831. Mortier, W. J.; Ghosh, S. K.; Shankar, S. *J. Am. Chem. Soc.* **1986**, *108*, 4315.

(26) Pearson, R. G. *J. Chem. Educ.* **1987**, *64*, 561; *Acc. Chem. Res.* **1993**, *26*, 250.

(27) Parr, R. G.; Chattaraj, P. K. *J. Am. Chem. Soc.* **1991**, *113*, 1854. Chattaraj, P. K.; Liu, G. H.; Parr, R. G. *Chem. Phys. Lett.* **1995**, *237*, 171. Pearson. R. G. *Chemtracts Inorg. Chem.* **1991**, *3*, 317. Liu, S.; Parr, R. G. *J. Chem. Phys.* **1997**, *106*, 5578. Chattaraj, P. K. *Proc. Indian Natl. Sci. Acad.-Part A* **1996**, *62*, 513. Pearson, R. G. *Chemical Hardness: Application from Molucules to Solids*; Wiley-VCH Verlag GMBH: Weinheim, 1997. Ayers, P. W.; Parr, R. G. *J. Am. Chem. Soc.* **2000**, *122*, 2010.

(28) Chattaraj, P. K.; Sengupta, S. *J. Phys. Chem.* **1996**, *100*, 16126.

(29) Ghanty, T. K.; Ghosh, S. K. *J. Phys. Chem.* **1996**, *100*, 12295.

(30) Chattaraj, P. K.; Sengupta, S. *J. Phys. Chem. A* **1997**, *101*, 7893.

(31) Chattaraj, P. K.; Poddar, A. *J. Phys. Chem. A* **1998** *102*, 9944; **1999**, *103*, 1274. Chattaraj, P. K.; Fuentealba, P.; Gomez, B.; Contreas, R. *J. Am. Chem. Soc.* **2000**, *122*, 348. Fuentealba, P.; Simon-Manso, Y.; Chattaraj, P. K. *J. Phys. Chem. A* **2000**, *104*, 3185. Chattaraj, P. K.; Fuentealba, P.; Jaque, P.; Toro-Labbe, A. *J. Phys. Chem. A* **1999**, *103*, 9307.

(32) Jaynes, E. T. In *Statistical Physics*; Ford, K. W., Ed.; Brandeis Lectures, Vol. 3; Benjamin: New York, 1963. Levine, R. D.; Bernstein, R. B. In *Dynamics of Molecular Collisions*; Miller, W. H., Ed.; Plenum Press: New York, 1976. Garde, S. R.; Bendale, R. D. *Curr. Sci.* **1985**, *54*, 970.

(33) Parr, R. G.; Szentpaly, L. v.; Liu, S. *J. Am. Chem. Soc.* **1999**, *121*, 1922.

(34) Chattaraj, P. K.; Sengupta, S. *J. Phys. Chem. A* **1999**, *103*, 6122.

(35) Chattaraj, P. K.; Nath, S. *Int. J. Quantum Chem.* **1994**, *49*, 705.

(36) Runge, E.; Gross, E. K. U. *Phys. Rev. Lett.* **1984**, *52*, 997. Dhara, A. K.; Ghosh, S. K. *Phys. Rev. A* **1987**, *35*, 442.

(37) Madelung, E. *Z. Phys.* **1926**, *40*, 322.

(38) Deb, B. M.; Ghosh, S. K.. *J. Chem. Phys.* **1982**, *77*, 342. Bartolotti, L. J. *Phys. Rev. A* **1982**, *26*, 2243.

(39) Gordy, W. *Phys. Rev.* **1946**, *69*, 604.

(40) Becke, A. D. *J. Chem. Phys.* **1986**, *84*, 4524.

(41) Ghosh, S. K.; Deb, B. M. *J. Phys. B* **1994**, *27*, 381.

(42) Brual, G.; Rothstein, S. M. *J. Chem. Phys.* **1978**, *69*, 1177.

(43) Ludena, E. V. *J. Chem. Phys*. **1983**, *79*, 6174. Kryachko, E. S.; Ludena, E. V. *Density Functional Theory of Many-Electron Systems*; Kluwer: Dordrecht, 1990.

(44) Polizer, P.; Parr. R. G.; Murphy, D. R. *J. Chem. Phys.* **1983**, *79*, 3859.

(45) Fuentealba, P. *J. Chem. Phys.* **1995**, *103*, 6571.

(46) Parr, R. G. *J. Phys. Chem.* **1988**, *92*, 3060.

(47) (a) Feit, M. D.; Fleck, J. A., Jr. *J. Chem. Phys.* **1984**, *80*, 2578. (b) Choudhury, S.; Gangopadhayay, G.; Ray, D. S. *Ind. J. Phys.* **1995**, *69B*, 507. (c) Graham, R.; Hohnerbach, M. *Phys. Rev. A* **1991**, *43*, 3966. (d) Idem. *Phys. Rev. Lett.* **1990**, *64*, 637.

(48) Pearson, R. G. *Chemical Hardness: Application from Molecules to Solids*; Wiley-VCH Verlag GMBH: Weinheim, 1997; pp 116−119.

(49) L'Huillier, A.; Lompre, L. A.; Mainfray, G.; Manus, C. In *Atoms in Intense Laser Fields*; Gavrila, M., Ed.; Academic Press: Boston, 1992; p 139.

(50) Clementi, E.; Roetti, C. *At. Data Nucl. Data Tables* **1974**, *14*, 174.

(51) Mukherjee, P. K.; Sengupta, S.; Mukherji, A. *Int. J. Quantum. Chem.* **1970**, *4*, 139.